Atlantic Basin Seasonal Hurricane Simulations

T. E. LARow, Y.-K. LIM, D. W. SHIN, E. P. CHASSIGNET, AND S. COCKE

Center for Ocean–Atmospheric Prediction Studies, The Florida State University, Tallahassee, Florida

(Manuscript received 14 May 2007, in final form 10 December 2007)

ABSTRACT

An ensemble of seasonal Atlantic hurricane simulations is conducted using The Florida State University/Center for Ocean–Atmospheric Prediction Studies (FSU–COAPS) global spectral model (Cocke and LaRow) at a resolution of T126L27 (a Gaussian grid spacing of 0.94°). Four integrations comprising the ensembles were generated using the European Centre for Medium-Range Weather Forecasts (ECMWF) time-lagged initial atmospheric conditions centered on 1 June for the 20 yr from 1986 to 2005. The sea surface temperatures (SSTs) were updated weekly using the Reynolds et al. observed data. An objective-tracking algorithm obtained from the ECMWF and modified for this model's resolution was used to detect and track the storms. It was found that the model's composite storm structure and track lengths are realistic. In addition, the 20-yr interannual variability was well simulated by the ensembles with a 0.78 ensemble mean rank correlation. The ensembles tend to overestimate (underestimate) the numbers of storms during July (September) and produced only one CAT4–level storm on the Saffir–Simpson scale. Similar problems are noted in other global model simulations. All ensembles did well in simulating the large number of storms forming in the Atlantic basin during 1995 and showed an increase in the number of storms during La Niña and a decrease during El Niño events. The results are found to be sensitive to the choices of convection schemes and diffusion coefficients. The overall conclusion is that models such as the one used here are needed to better hindcast the interannual variability; however, going to an even higher resolution does not guarantee better interannual variability, tracks, or intensity. Improved physical parameterizations, such as using an explicit convection scheme and better representation of surface roughness at high wind speeds, are likely to more accurately represent hurricane intensity.

1. Introduction

Manabe et al. (1970) were the first to show that a low-resolution general circulation model (GCM) could simulate hurricane-type vortices (HTVs). Because of the resolution of the GCM, the storm structure tended to be much larger and weaker than observed with characteristic scales on the order of 2000–4000 km. As computing power and our knowledge of tropical systems increased, so have our ability to simulate HTV in current GCMs. Bengtsson et al. (1982, 1995, 2007a), Broccoli and Manabe (1990), and Haarsma et al. (1993) have all shown that one can perform seasonal hindcasting of tropical storm activity (i.e., simulations with observed sea surface temperatures) a season or more in advance using models of various horizontal resolutions and that the HTVs have a climatology and physical structure similar to the observed.

The basic idea of seasonal hindcasting of tropical storms is related to the idea that tropical storm activity is closely tied to characteristics of the large-scale circulation, sea surface temperatures (SSTs), horizontal–vertical shear, and low-level vorticity (e.g., Gray 1979). Most of the time changes in the large-scale features can have a pronounced impact on the variability of Atlantic tropical storm activity. For example, during an El Niño, the number of tropical storms in the Atlantic tends to be reduced (Gray 1984; Shapiro 1987). It is these large-scale features that the GCM is able to reproduce reasonably well, thereby allowing GCMs and coupled ocean–atmosphere models (e.g., Vitart et al. 2007) to be used to hindcast/forecast tropical cyclone activity. However, because coupled ocean–atmosphere models drift from the observed climate, their bias has to be removed from the model's solution, a posteriori. For example, in the study by Vitart et al. (2007), their coupled climate model tended to produce too many

Corresponding author address: T. E. LaRow, Center for Ocean–Atmospheric Prediction Studies, The Florida State University, Tallahassee, FL 32306-2840.
E-mail: tlarow@coaps.fsu.edu

DOI: 10.1175/2007JCLI2036.1

storms, thus they had to apply a multiplication factor to the number of storms generated by the model for the median of the model's climate to be equal to the medium of the observed climate. In addition, the components of a coupled model have to be initialized together to reduce initial coupled shock to the system (LaRow and Krishnamurti 1998). This is especially true for short-term seasonal forecasts where imbalances in the coupled system manifest themselves the fastest.

The exact reason for the genesis of warm-core features in GCMs has been called into question (Evans 1992; Lighthill et al. 1994) because of these features' sensitivity to the vertical wind shear. However, the interannual variability of modeled tropical storms has been found to be consistent with observations (Vitart and Stockdale 2001).

This study uses an ensemble of seasonal integrations (June–November) produced using The Florida State University–Center for Ocean–Atmospheric Prediction Studies (FSU–COAPS) global spectral model at a horizontal resolution of T126L27 (a Gaussian grid spacing of 0.94°) to hindcast the western Atlantic basin tropical storm activity for the 20-yr period of 1986–2005. This paper examines whether the use of increased horizontal resolution improves the seasonal Atlantic hurricane hindcasts in terms of tracks, intensities, frequencies, and interannual variability. While there has been GCM studies that use higher horizontal resolution (e.g., Bengtsson et al. 2007a,b; Oouchi et al. 2006), the work reported here shows that one cannot discard the significance of the choices made for the dissipation coefficients and for other physical parameterizations.

This paper is divided into the following six sections: section 2 discusses the model and the experimental setup. The detection and tracking algorithm is discussed in section 3. Section 4 discusses the results. Some sensitivity to the choice of convection scheme and diffusion coefficients is briefly discussed in section 5. Summary and conclusions are presented in section 6.

2. Model and experiments

The FSU–COAPS model (Cocke and LaRow 2000) was used in this study. The resolution of the model was T126 with 27 vertical levels (T126L27). A relaxed Arakawa–Schubert deep convection scheme (Hogan and Rosmond 1991) was employed in the experiments. A total of 80 experiments were conducted with four ensemble members for each of the 20 yr (1986–2005). The time-lagged initial conditions for the atmospheric model were obtained from the European Centre for Medium-Range Weather Forecasts (ECMWF) reanalysis and were centered on 1 June of the respective year. The integrations for the 6-month period (June–November) were conducted to coincide with the Atlantic basin hurricane season. The observed SSTs were obtained from the Reynolds et al. (2002) dataset and were updated once per week using daily linear interpolation between the weeks.

3. Detection and tracking algorithm

Identifying interannual tropical storm variability can be divided into three methods. The first method uses statistical techniques (Gray et al. 1992, 1993, 1994; Hess et al. 1995; and others). The second method uses seasonal genesis parameters, which are known to affect tropical cyclone activity (Ryan et al. 1992; Watterson et al. 1995; Thorncroft and Pytharoulis 2001). The third approach, and the one used in this paper, detects and tracks the simulated tropical cyclone activity directly from the dynamical model's output.

The detection algorithm used here is similar to the one used by Vitart et al. (2003) and Knutson et al. (2007) but was modified slightly for our model's resolution. The detection algorithm is based on three criteria. First, a local vorticity maximum greater than 4.5×10^{-5} s^{-1} is located at 850 hPa. Second, the closest local minimum in sea level pressure is detected and defines the center of the storm. This must exist within a $2° \times 2°$ radius of the vorticity maximum. Third, the closest local maximum temperature is detected between 500 and 200 hPa and defines the warm core. The distance between the center of the storm and the center of the warm core must not exceed 2° latitude. From the center of the storm, the temperature must decrease by at least 6°C in all directions within a distance of 4°. For our study, we increased the vorticity threshold from 3.5×10^{-5} to 4.5×10^{-5} s^{-1} and also increased the warm-core temperature maximum from 0.5° to 6°C. This was done to help reduce the number of false alarms detected because of the model's horizontal resolution while still identifying most tropical systems.

Trajectories must last more than 2 days and have the lowest model–level wind velocity within an 8° radius circle centered on the storm center that is greater than 17 m s^{-1} during at least 2 days (does not have to be consecutive days).Using the threshold of 17 m s^{-1}, it is possible that we could be underestimating the number of storms (Walsh et al. 2007). The criteria for detection is partly subjective and partly to agree with other GCM studies. In contrast to the Camargo and Zebiak (2002) detection algorithm, which is dependent upon both the model's resolution and basin, the Vitart algorithm is based only on the model's resolution. In this paper, the observed tropical storms for the June–November time period are identified according to the National Hurri-

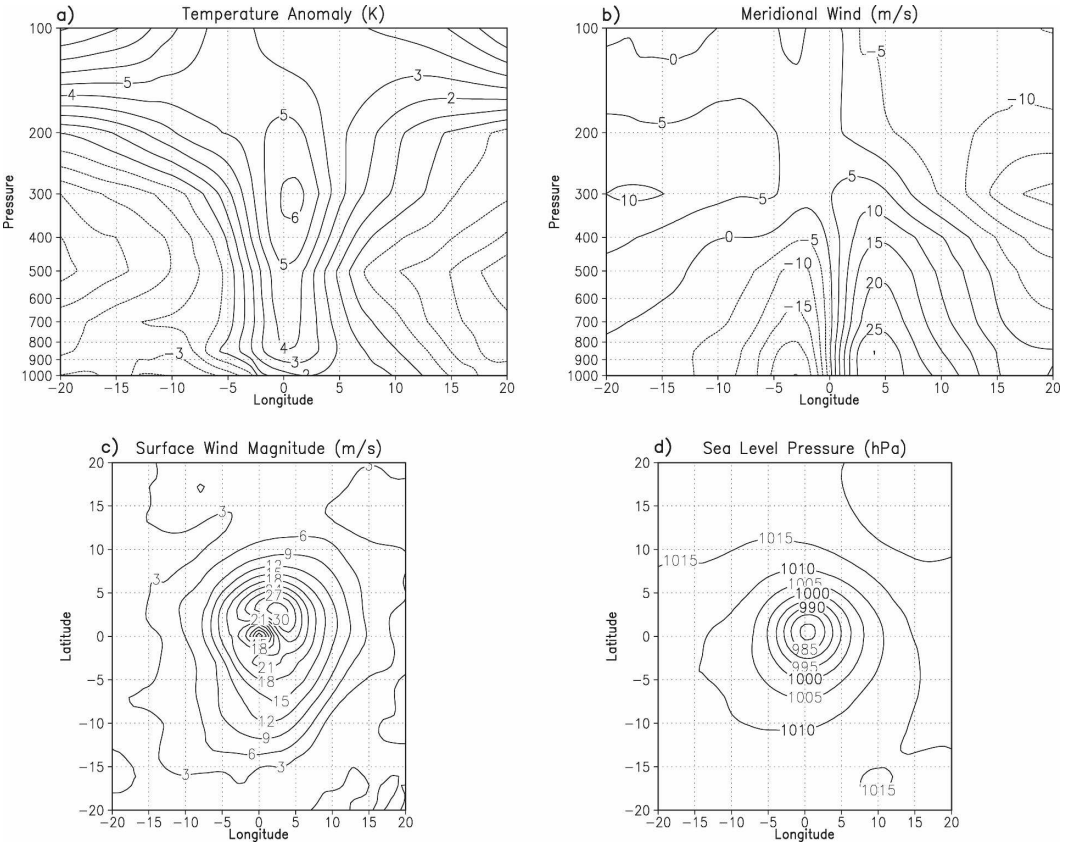

FIG. 1. An FSU–COAPS model's tropical storm composite including (a) temperature anomaly cross section through the center of the storm's composite (K), (b) meridional wind cross section through the center of the storm's composite (m s^{-1}), (c) composite surface wind magnitude (m s^{-1}), and (d) composite sea level pressure (hPa).

cane Center Best Track dataset, HURDAT (available online at http://www.nhc.noaa.gov/pastall.shtml).

4. Results

a. Hurricane-type vortice structure

Before examining the model's ability to simulate interannual variations of hurricanes in the Atlantic basin, we will first discuss the model's ability to simulate HTVs. Several studies (e.g., Wu and Lau 1992; Bengtsson et al. 1995; Chauvin et al. 2006; McDonald et al. 2005; Vitart et al. 1997) have all shown various horizontal resolutions of hurricane-like features, that is, convergence at low levels, divergence at upper levels, large amounts of precipitation, and high relative humidities. These HTV features are dependent on the model's resolution—the coarser the resolution, the larger the HTV tends to be (Bengtsson et al. 1995).

Figures 1a and 1d show a composite of 42 storms from the ensembles taken at their maximum intensity. Storms chosen for the composite had to have their maximum intensity occurring south of 30°N to avoid any influences of extratropical transition. The latitudes and longitudes are shown on the plots to give size representation and do not represent actual positions. These composites were generated by first locating the storm's center and then taking a radius of 20° around it. Figure 1a shows the average temperature anomaly cross section from west to east through the center of the composite storm. The warm-core temperature anomaly of 6 K is located near 300 hPa. Slightly warmer anomalies are found near 100 hPa, while colder anomalies are located on either side of the warm core. Figure 1b shows the average meridional wind cross section through the center of the storms from west to east. Low-level cyclonic flow is seen with maximum winds greater than 25 m s^{-1} located near 850 hPa and decreasing toward lower pressure. Above 300 hPa the meridional wind reverses and anticyclonic winds are found, an indication of good ventilation in the composite storm. Figure 1c shows the surface wind field with maximum winds of greater than 30 m s^{-1} located in the northeast

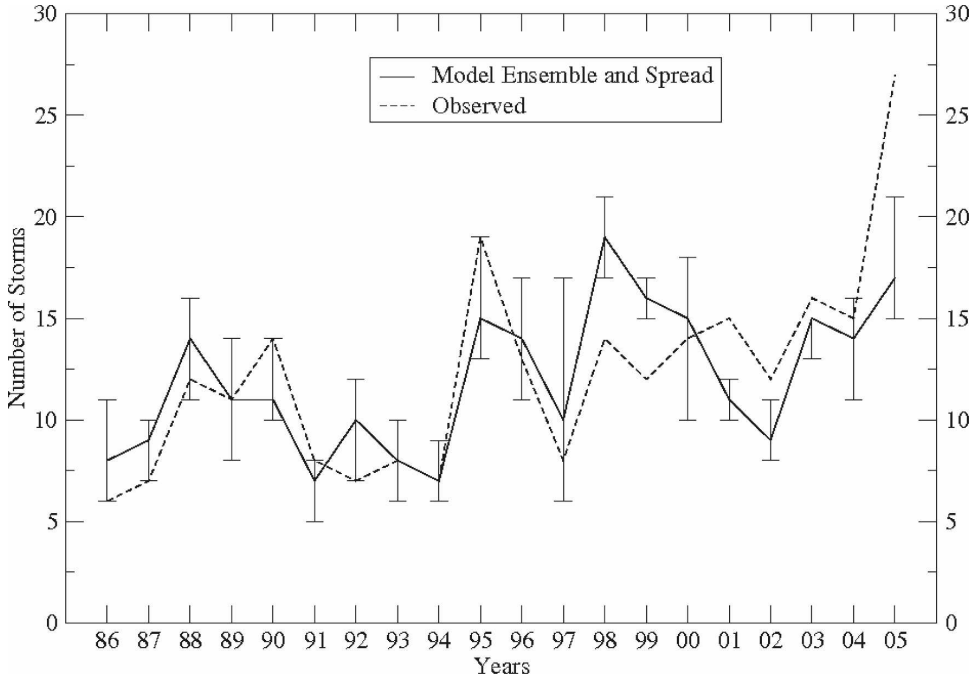

FIG. 2. Interannual variability of tropical storms from 1986 to 2005 including the observations (dotted line), the ensemble mean (solid line), and the ensemble spread (vertical lines).

quadrant of the storm composite. The quasi-axisymmetrical appearance of the surface pressure (Fig. 1d), with a minimum surface pressure of 980 hPa, is found in the composite storm's center. Both surface winds and surface pressure composite indicate a category 1 storm on the Saffir–Simpson scale. These results should be seen as mainly qualitative since the Saffir–Simpson winds are based on 1-min sustained surface wind speeds and our model's output is once every 6 h.

b. Atlantic basin interannual variability

The number of storms for each year from each ensemble is calculated from the detection algorithm, and the ensemble mean and spread are plotted along with the observed as a function of year in Fig. 2. No rescaling of the figure was done. The observed number of storms (from HURDAT for the June–November time period) is shown with the dotted line, while the ensemble mean and spread are shown with the solid line. The spread of the ensembles is shown with the vertical lines. Overall, the ensemble mean does well in simulating the interannual variations in the storm numbers, except during the cold ENSO event years of 1998 and 1999, when the ensemble mean is higher than the observed. In addition, the model was unable to simulate the record number of 27 storms during 2005, but instead simulated a maximum of 21 storms.

The spread of the ensembles was largest during the warm ENSO event of 1997 (a spread of 11 storms), although the ensemble mean was only two storms away from the observed. As stated by Wu and Lau (1992), El Niño tends to reduce the number of tropical storms in the Atlantic, but during La Niña the opposite occurs. This pattern of a reduced number of storms during the warm events and an increased number during the cold events is clearly seen in the ensemble mean. The model might be sensitive to the ENSO state, but with such a small record length and ensemble size it is difficult to be certain. The model did well in simulating the record number of storms during 1995.

The 20-yr rank correlation of the ensemble mean with the observed was 0.78. The observed standard deviation was 5.02 for the 20 yr of the study, while the standard deviation of the ensemble mean was slightly lower at 3.54, although ensembles 1 and 4 show standard deviations much closer to the observed, with values of 4.49 and 4.24, respectively (see Table 1). The high correlation noted is most likely related to the use of weekly observed SSTs and the choice of the convection scheme (discussed briefly in section 5). Table 1 shows the individual ensemble correlations, standard deviations, and the total number of storms for the entire 20-yr period. Studies by Gray (1984), Shapiro (1987), and Saunders and Harris (1997) all show that

TABLE 1. Shows total number of storms, rank correlations, and std dev during the 20-yr period from the observed and each ensemble.

	Observations	Ensemble 1	Ensemble 2	Ensemble 3	Ensemble 4
Total storms	245	242	234	234	249
Correlation		0.72	0.62	0.69	0.64
Std dev	5.02	4.49	3.6	4.24	3.86

the SSTs can have a significant impact on the tropical storm statistics, especially in the Atlantic.

c. Frequency

The observed and ensemble frequencies of the number of storms per month are shown in Fig. 3. The frequency is in respect to the annual cycle, although we only show that portion of the annual cycle contained in our study. The observed monthly frequency (solid line) is calculated from the 20 yr of the study. The observed shows a small increase in the number of storms from June to July and then a large increase in August, with a peak in September followed by a sharp decline moving toward November. Although all four ensembles (dashed lines) overestimate the number of storms in July and underestimate the storms during September, the number of storms is in good agreement with the observed, something that is not found in previous studies (e.g., Camargo and Zebiak 2002, Fig. 7a; Camargo et al. 2005, Fig. 6d). Although these studies underestimated the number of tropical systems, they did, however, predict the maximum during September. Similar findings by Vitart et al. (1997) show a maximum number of storms occurring during September with an overestimate during July and a slight underestimate during September. All of these studies were with low-resolution models (T42), indicating that higher resolution (as shown in this study) does not guarantee the correct frequency distribution, but it might help with the magnitude of the distribution. Annual frequency distribution seems to be more a matter of the model's physics than of the model's resolution. The individual members of the ensemble all show the observed decline in storm activity from October to November.

d. Accumulated cyclone energy

Examination of the seasonal accumulated cyclone energy (ACE) from the ensemble mean and the observations for each year is shown in Fig. 4. Seasonal ACE is defined as the sum of the square of the winds during

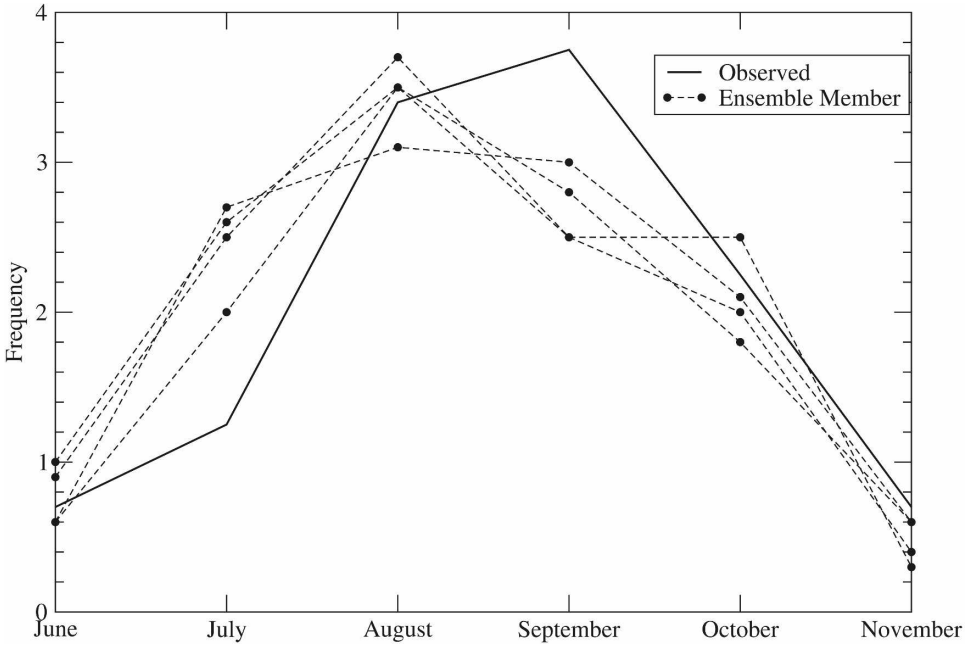

FIG. 3. Frequency of tropical storms for (June–November) 1986–2005 including the observation (solid line) and individual ensemble members (dotted lines).

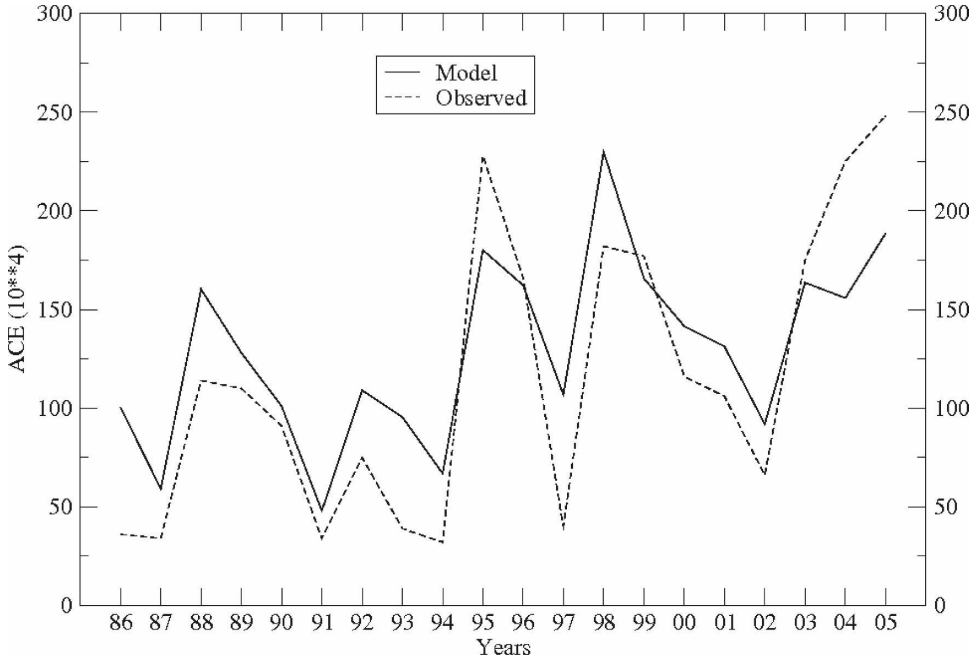

FIG. 4. Atlantic ACE including the model's ensemble mean (solid line) and the observation (dashed line) in 10^4 kts^2 for all 20 yr of the hindcast.

the lifetime of each storm that has accumulated during the season. In determing the model's ACE, the 850-hPa winds are used because the detection algorithm uses the 850-hPa wind fields to determine the storm's center and lifetime. The rank correlation with the observed ACE is 0.85. The only year that the model and observed ACE do not agree in the tendency is 2004; the model shows a decreasing trend while the observed data shows an increasing trend. The model overestimates the ACE index during the first 9 yr of the study, which agrees with the model's overestimate of storm activity shown in Fig. 2. Underestimates are found during the years 1995 and 2005, with both being very active years in the observations but underestimated by the model's ensemble mean (Fig. 2). It is possible that the ACE values from the model could be underestimated because the detection algorithm requires that a 6-K temperature anomaly be found before we start tracking the model's storms. This requirement could limit the lifetime of the model's storms and lead to lower ACE values.

e. Wind–pressure relationship

A scatter diagram of the Atlantic HTV surface wind versus surface pressure relationship in all 80 ensemble members and its associated observed HURDAT wind–pressure relationship are shown in Fig. 5. This shows that the model cannot generate storms with surface wind speeds greater than 50 m s^{-1}, while the observations show surface pressures as low as 882 hPa [Hurricane Wilma (2005)] and surface wind speeds of 82 m s^{-1} [Hurricanes Gilbert (1988) and Wilma (2005)]. The model's surface winds were determined by multiplying the 850-hPa winds by 0.80 to reduce the surface winds. The value of 0.80 is commonly applied to flight-level winds (typically 850 hPa) to estimate surface wind speeds (see www.nhc.noaa.gov/aboutwindprofile.shtml). The model's lowest surface pressure was 936 hPa and the highest surface winds were 47 m s^{-1}. It is interesting to note that the model's minimum in surface pressure was not associated with the maximum wind.

Individual storm intensity is still a problem because of insufficient horizontal resolution. Similar difficulties in producing intense storms using even higher-resolution models than were used in this study were noted by Bengtsson et al. (2007a), Knutson et al. (2007), and Oouchi et al. (2006). In another study, Bengtsson et al. (2007b) used two models of an even higher horizontal resolution than was found in Bengtsson et al. (2007a) and noted increased intensity; however, they warn that the increase might be because of the lack of coupling to an ocean model, which would provide for negative feedbacks on the storm's intensity. All of these studies indicate that the model's resolution—and perhaps the model's physics—are still insuf-

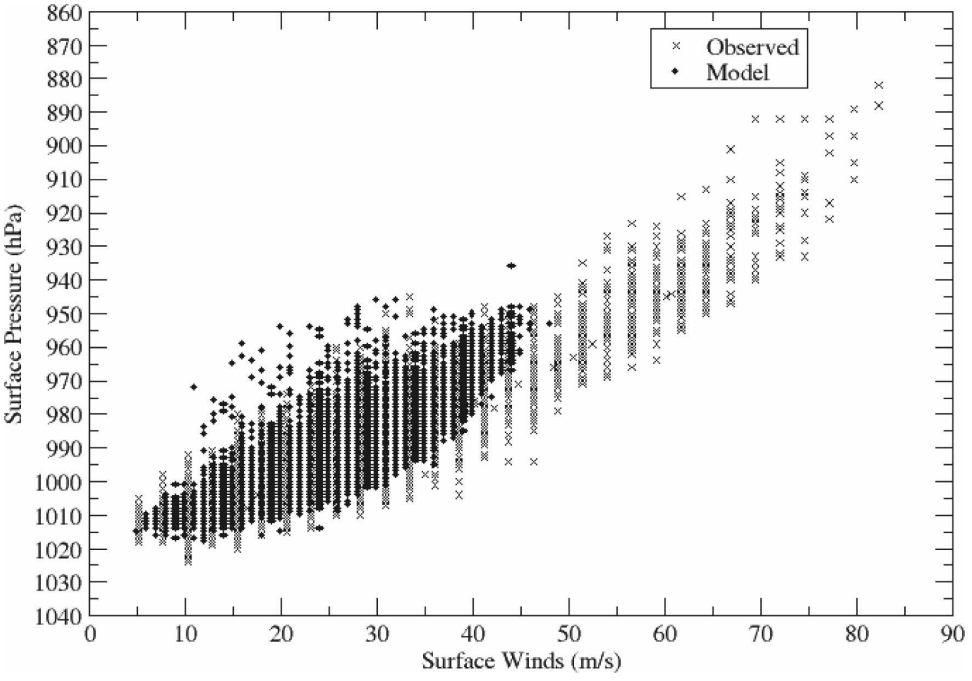

FIG. 5. Model and observed HURDAT surface wind–pressure relationship including the model ensembles (solid circles) and the HURDAT dataset (hatched crosses). All 80 ensemble members are shown for all 20 yr of the study.

ficient when it comes to storm intensity. Switching the physical parameterization schemes and/or using an explicit convection scheme might yield more intense storms. Some insight might be gleaned from examining integrations with a cloud-resolving model, such as the National Aeronautics and Space Administration (NASA) finite element model (Atlas et al. 2005). This model has been run at a horizontal resolution of 0.25° and appears to show realistic hurricane surface pressures/deepening rates and tracks when integrated out to 5 days.

f. Storm tracks

All storm tracks for the entire 20 yr for the months of June–November from ensemble 1 and the observed HURDAT data are shown in Figs. 6a and 6b. The observed total number of storms for that period was 245, and this ensemble identified 242 storms (see Table 1). This close similarity of the ensemble members to the observed number is in contrast to other modeling studies that underestimate the number of tropical storms in the Atlantic (e.g., Camargo and Zebiak 2002; Bengtsson et al. 2007a; and Vitart 2006). Similar tracks from the other ensembles are not shown because they are very similar to those seen in Fig. 6a.

The model generates most of the storms near 10°N, 45°W with a general west-to-northwest track (Fig. 6a). Most of the model's storms recurve toward the northeast before coming close to the North American east coast, with only a few storms making landfall along the east coast of the United States. The model's tracks are in contrast to the observed tracks (Fig. 6b), which show a more westward movement toward the United States before recurving northward and, consequently, many more storms striking the eastern United States in the observations. In addition, observations show that more storms tend to form closer to Africa. The model produced more landfalling storms along the Gulf of Mexico coastline than along the eastern seaboard, especially along the northern Florida coastline, but, again, too few compared to the observations. The model's detection algorithm identified a few storms forming north of 30°N latitude. These storms are probably polar lows, which are known to have high low-level vorticity, minimum surface pressure, strong surface wind speeds, short lifetimes, and a warm-core structure, thereby, they satisfy the detection criteria. The longest duration of a model's storm from all ensemble members was 19.5 days, while the average model's storm duration was close to 5 days. Observations show that the average duration of an Atlantic tropical system is 6 days. Vitart et al. (1997) found that their average storm duration was 4 days.

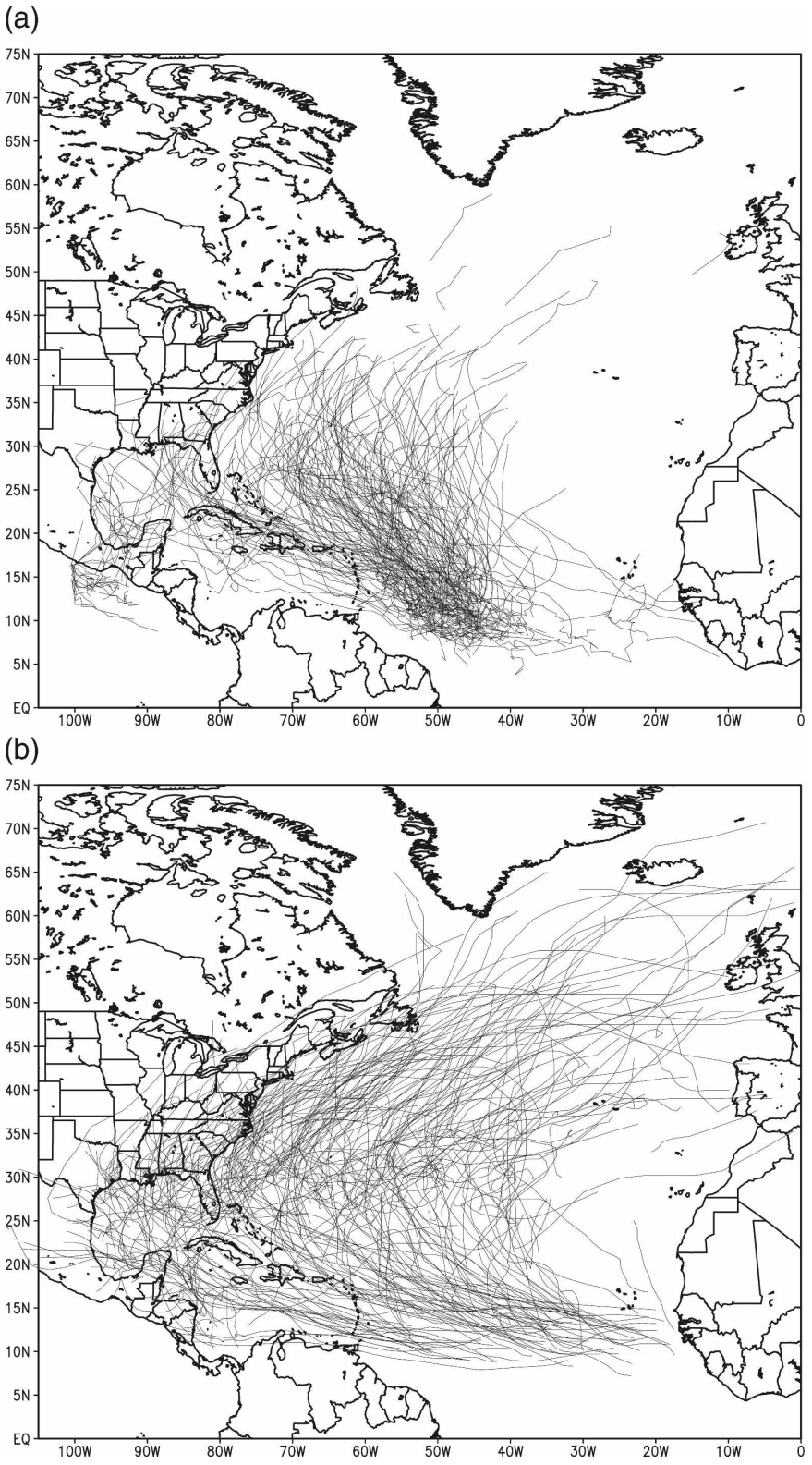

FIG. 6. Storm tracks for the entire hurricane season (June–November) for 1986–2005 including (a) from ensemble member 1 and (b) observed storm tracks from the HURDAT dataset. Other ensembles are not shown because the tracks are similar among ensemble members.

TABLE 2. Number of storms impacting different sections of the United States from each ensemble using the Hogan and Rosmond (1991) convection scheme and the HURDAT dataset for (June–November) 1986–2005. Mid-Atlantic area includes the states of SC, NC, VA, MD, DE, and NJ. The New England area includes the states of NY, CT, RI, MA, NH, and ME. Landfalling storms are only counted one time during their first landfalling event. Multiple landfalling events [e.g., Katrina (2005)] are only counted once.

Gates	Ensemble 1	Ensemble 2	Ensemble 3	Ensemble 4	HURDAT
TX	8	14	10	4	36
MS/LA	3	3	2	5	11
FL/GA/AL	23	17	17	15	33
Mid-Atlantic	2	4	5	2	11
New England	2	4	5	2	11

By placing "gates" around the United States and counting the number of storms making landfall in a particular gate of the United States, the lack of landfalling storms along the East Coast is clearly evident (Table 2). We have developed five such gates according to the model's land–sea mask: Texas, Louisiana–Mississippi, Florida–Georgia–Alabama, the mid-Atlantic area, which includes South Carolina north to Delaware, and the New England area, which includes New York north to Maine. Storms are only counted making landfall once. For example, storms such as Hurricane Katrina (2005), which made landfalls in south Florida then again in Louisiana in the observations, are only counted once; in this case, Katrina is counted as making landfall in Florida. This method of counting was done for all ensembles and the HURDAT observations using the land–sea mask from the model. The number of storms from ensemble 1 that made landfall along the Texas–Louisiana border was only eight, while in the HURDAT observational dataset there were 36 during the 1986–2005 hurricane season. Similarly, along the Florida–Georgia border there were 22 storms that made landfall in ensemble 1, while observations show 33. Northward into the mid-Atlantic states and the New England states the problem of recurvature becomes more pronounced with ensemble 1 only showing 3 and 2 storms, respectively, while the observations show there were 11 storms impacting both locations.

The 500-hPa streamlines for 1986–2002 were used to examine the discrepancy in the model's tracks for ensemble 1 as compared to the ECMWF reanalysis. The streamlines for all 20 yr from ensemble 1 are shown in Figs. 7a and 7b. For examination purposes, because the model's hurricanes peak in August, the hurricane season was divided into two parts: June–August (JJA; Fig. 7a) and September–November (SON; Fig. 7b). Similar streamline plots from the ECMWF reanalysis are shown in Figs. 7c and 7d. During the first half of the hurricane season (Fig. 7a), the model's 500-hPa streamlines show a break in the subtropical ridge located over the center of the Atlantic. This break in the ridge enables the tropical systems to move poleward before they impact the United States. In contrast, the Bermuda high is clearly evident in the ECMWF reanalysis (Fig. 7c) during June–August.

During the second half of the hurricane season (Figs. 7b,d), the 500-hPa streamlines continue to be poorly simulated by the ensemble mean compared to the ECMWF reanalysis. The high pressure situated over Cuba in the reanalysis is located farther to the west over Mexico in the ensemble.

g. 200-hPa velocity potential and SST anomalies

Examination of the 200-hPa velocity potential and divergent wind from the ensemble mean and the ECMWF reanalysis for July–September (JAS) for the years 1986 and 1995 are examined for large-scale influences on the tropical cyclone activity. These years were chosen because they represent an inactive year (1986) and an active year (1995) in terms of Atlantic hurricane activity. SST anomalies' patterns and their associated large-scale atmospheric circulation patterns must be examined when considering the number of tropical cyclones (Chauvin et al. 2006). During JAS 1986, the observed SST anomalies in the tropical Atlantic and Gulf of Mexico were dominated by negative anomalies, and the tropical eastern Pacific (west of 120°W) shows slightly warm anomalies (Fig. 8a). This type of pattern sets up a weaker Walker circulation and a stronger Hadley circulation, which helps to limit the number of Atlantic storms that can form. During JAS 1995, the opposite is true for the SST anomalies in both basins (Fig. 8b), with warm tropical Atlantic and Gulf of Mexico temperatures and cold anomalies in the tropical Pacific. This distribution of SST anomalies helps to set up a stronger Walker circulation and a weaker Hadley circulation, resulting in more favorable conditions for Atlantic hurricane activity. The months of July–September were chosen because they correspond to the period of most activity in the Atlantic basin, both in terms of observed climatology and in the model simulations. The observed number of tropical systems

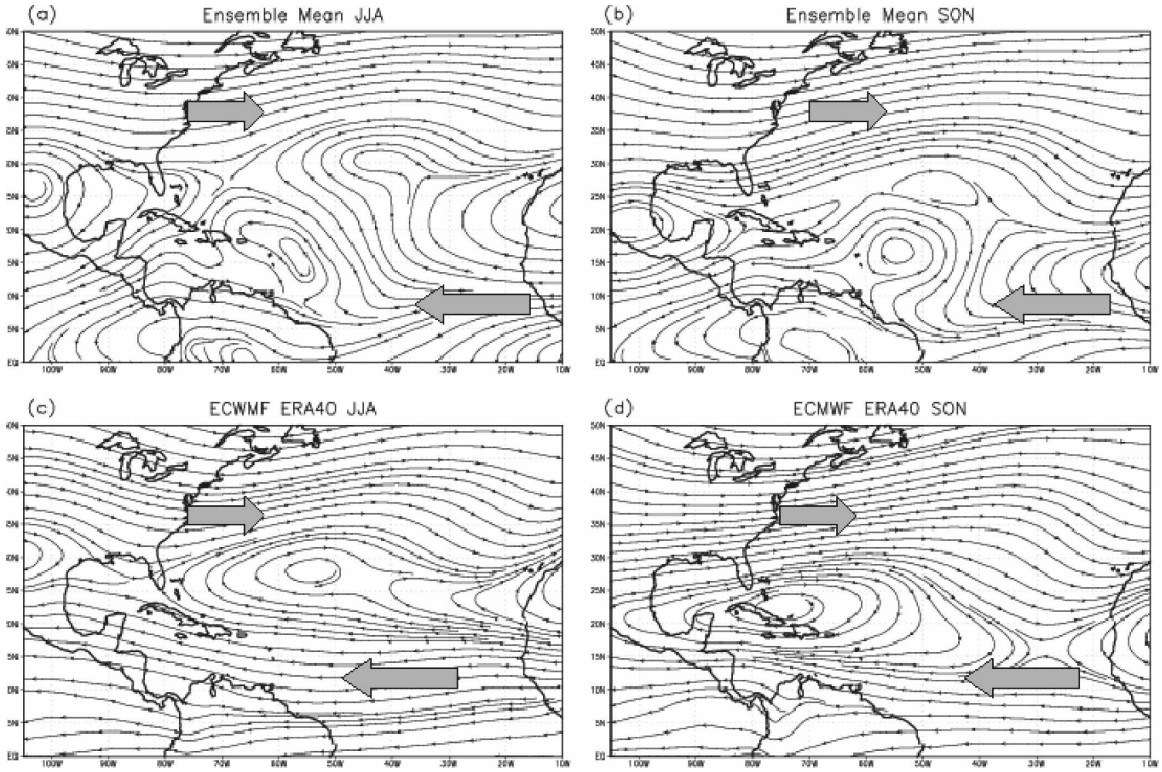

FIG. 7. The 500-hPa streamlines for 1986–2001 include (a) JJA ensemble mean from ensemble 1 using the Hogan and Rosmond (1991) convection scheme, (b) SON ensemble mean from ensemble 1 using the Hogan and Rosmond (1991) convection scheme, (c) JJA ECMWF reanalysis, and (d) SON ECMWF reanalysis.

during 1995 was 19 (11 hurricanes), while the ensemble mean produced 15 tropical storms/hurricanes (see Fig. 2).

During the weak event year of 1986, the ensemble mean shows a broad area of weak upper-level divergence located over the central Atlantic with convergence over the southern Indian Ocean (Fig. 9a). Strong divergence is also noted over the western Pacific and the north Indian Ocean, which is associated with the warm ocean temperatures and the Asian summer monsoon. The corresponding ECMWF reanalysis (Fig. 9b) shows the climatological divergent pattern over the Gulf of Mexico–Central America region. Convergence is found in the reanalysis over the eastern Atlantic, which helps to suppress tropical storm activity. The ensemble mean failed to simulate any convergence over the Atlantic and despite the upper-level divergence, the ensemble mean only generated a total of eight tropical systems during 1986 (see Fig. 2).

During JAS 1995, there were 14 named storms (7 hurricanes) observed in the Atlantic. Figure 9c shows the ensemble mean 200-hPa velocity potential and divergent wind. A stronger divergent pattern, compared to 1986, is noted in the ensemble mean and is associated with a more favorable environment for an increase in tropical activity during 1995. Weak upper-level convergence noted over the eastern Atlantic in the ECMWF reanalysis during 1986 is absent during 1995 (Fig. 9d). The model ensemble divergence is much stronger than that found in the ECMWF reanalysis during this period; however, with this stronger divergence the model was able to generate an increase in tropical storm activity compared to 1986. The stronger divergence found in the ensemble mean is likely because of an overestimation of persistent tropical Atlantic convection in the model (not shown). This area of convective activity corresponds to regions where the tropical storm detection seems to occur most frequently (see Fig. 6a).

5. A note on convection schemes and diffusion coefficients

Two other convective schemes were tried. Both convection schemes were developed at U.S. meteorological centers. Only one experiment each for the 20-yr period for both convection schemes were conducted. The results varied considerably with one of the convection schemes, a simplified Arakawa–Schubert scheme (Pan

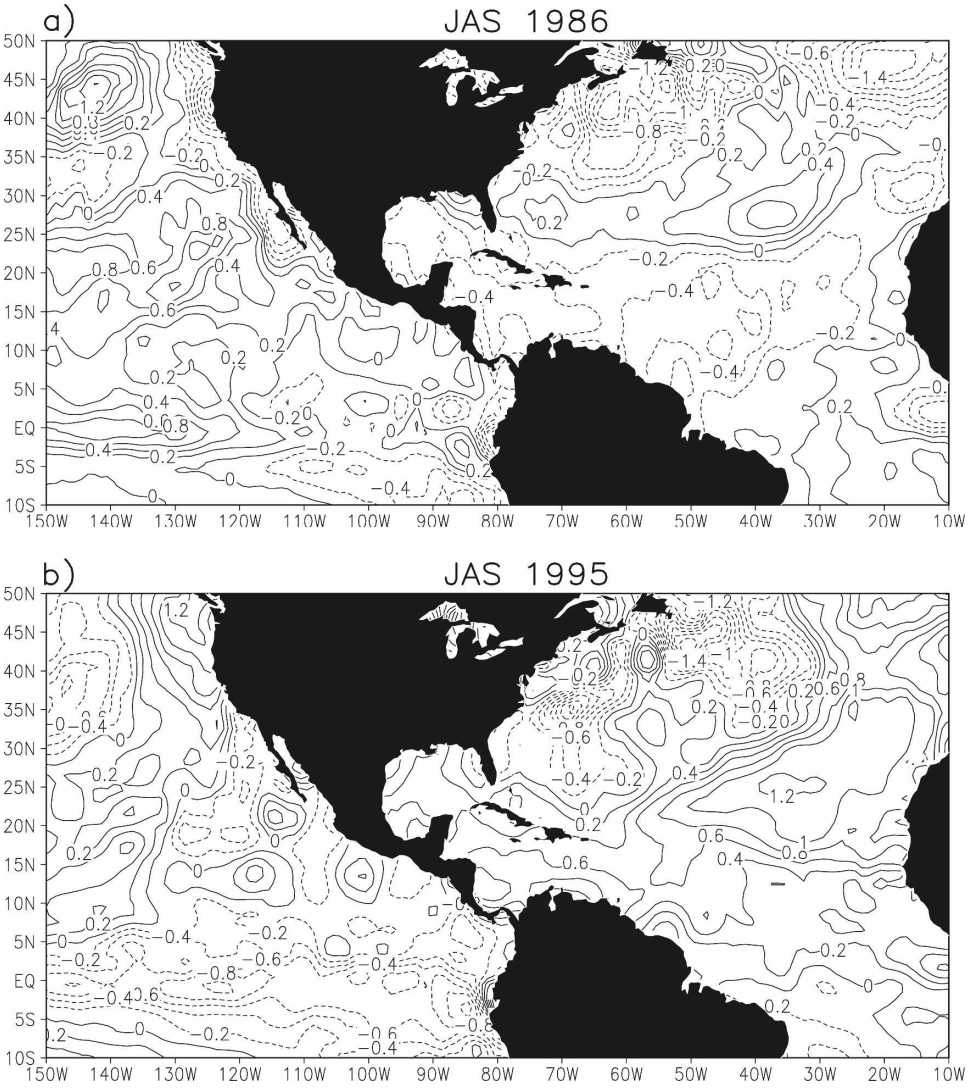

FIG. 8. Observed SST anomaly from Reynolds et al. (2002) includes (a) July–September 1986 and (b) July–September 1995. The contour interval is 0.2°C.

and Wu 1994), failing to produce any storms during the 20-yr period. This could perhaps be related to the stringent requirements for the detection of a tropical storm used in this paper. It is possible that by using weaker warm-core detection criteria, this convection scheme could have developed some tropical systems.

The other convection scheme, a relative humidity and Convective Available Potential Energy (CAPE) threshold scheme from the National Center for Atmospheric Research (NCAR; Zhang and McFarlane 1995), produced too many storms during La Niña years (more than 30 storms in 1988, 1998, and 1999), and its correlation with the observed interannual variability was significantly lower (−0.01) than the results shown in Fig. 2. It is interesting to note that while the correlation of the interannual variability in the number of tropical systems identified from the NCAR convection scheme was lower than any of the ensembles shown in Fig. 2, the NCAR scheme did simulate the 500-hPa wind fields much closer to the ECMWF reanalysis (Fig. 10). As a result, the NCAR scheme simulates better landfalling statistics (see Table 3), especially in the mid-Atlantic and New England regions (12 storms in each region compared to the observed of 13). This is partly a result of the better 500-hPa steering flow and the fact that the NCAR scheme produced approximately 30% more total storms than was found in any of the control ensembles.

The choice of convection scheme in our model was found to be important in determining the large-scale

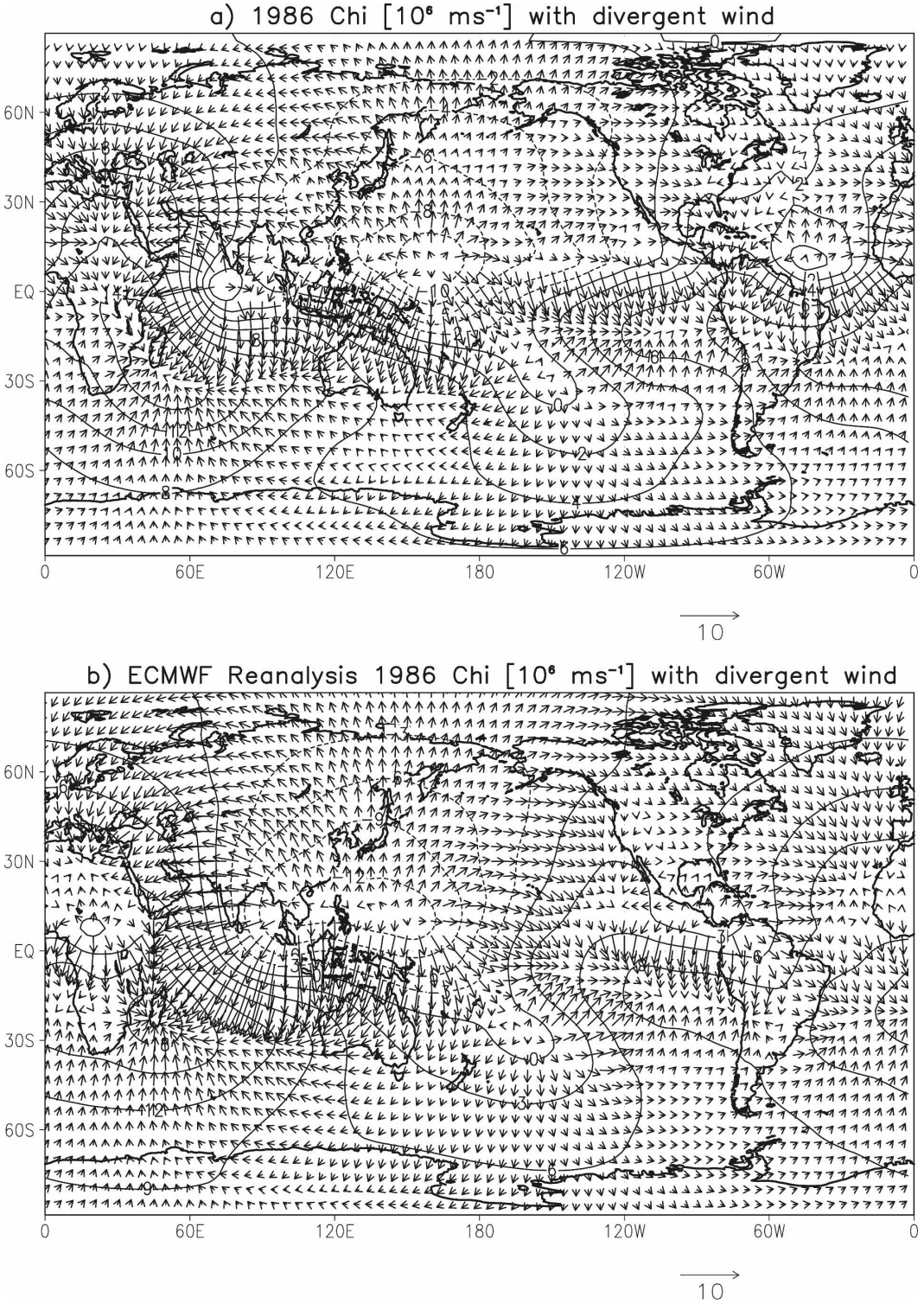

FIG. 9. JAS velocity potential and divergent wind include (a) 1986 ensemble mean, (b) 1986 ECMWF reanalysis, (c) 1995 ensemble mean, and (d) 1995 ECWMF reanalysis, and they show an inactive Atlantic hurricane season in 1986 and an active season in 1995.

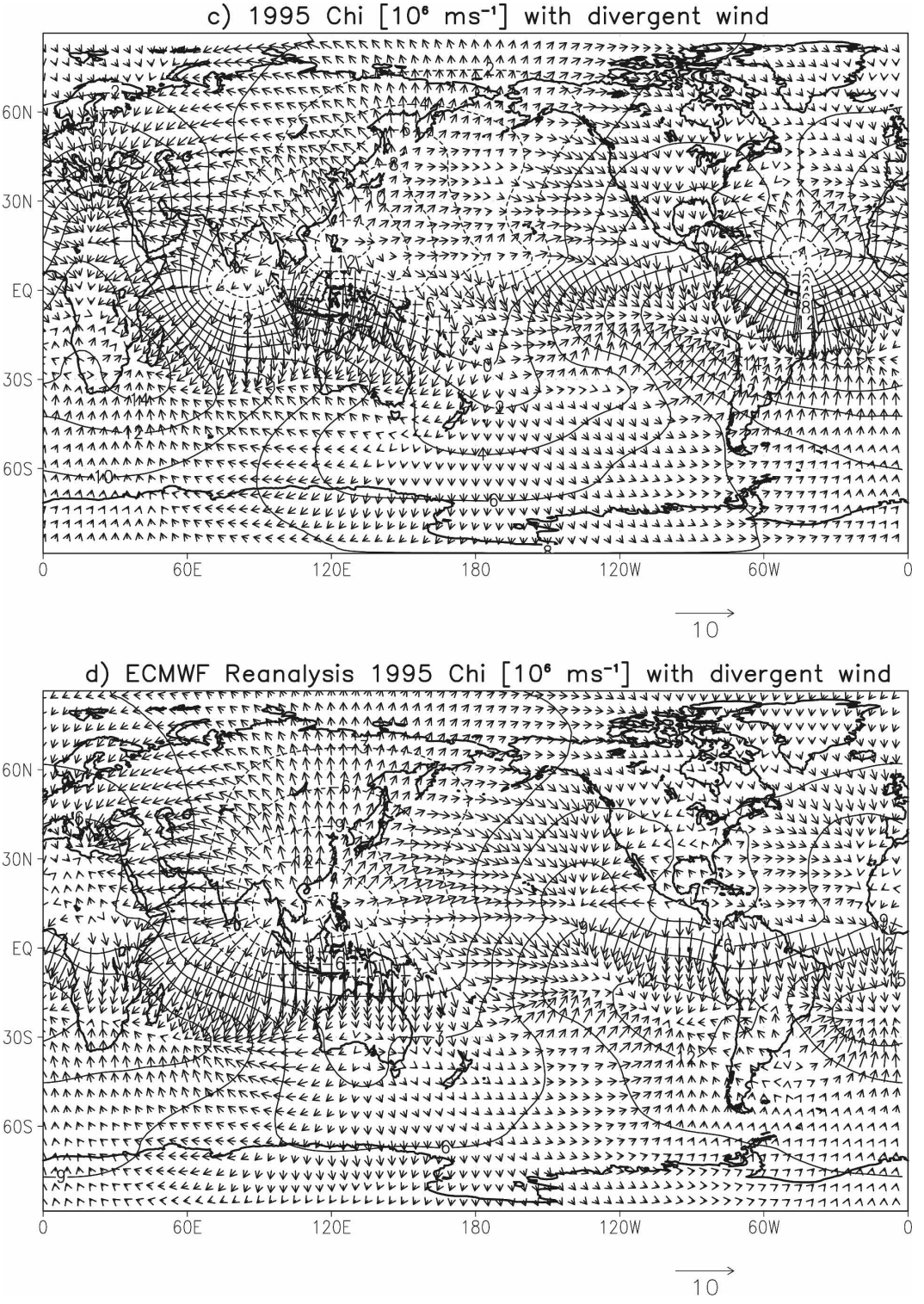

FIG. 9. (*Continued*)

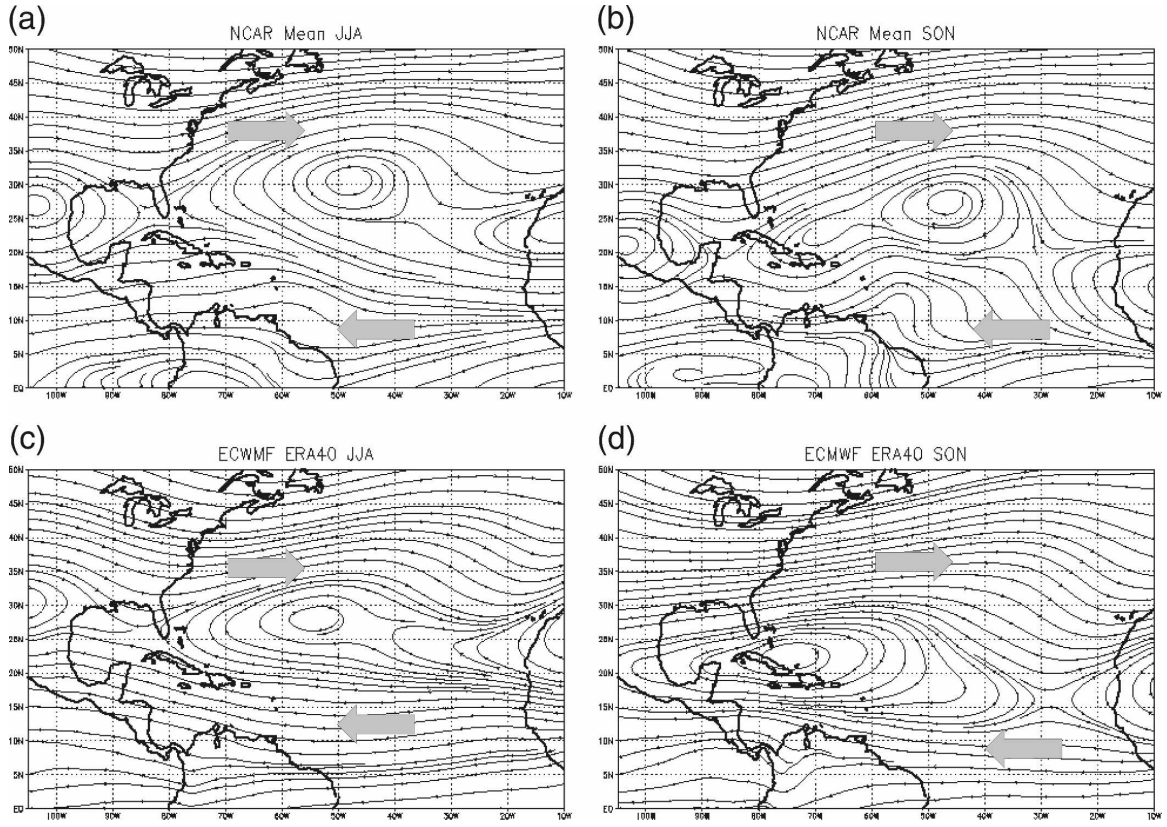

FIG. 10. The 500-hPa streamlines for 1986–2001 include (a) JJA ensemble mean using the Zhang and McFarlane (1995) convection scheme, (b) SON ensemble mean using the Zhang and McFarlane (1995) convection scheme, (c) JJA ECMWF reanalysis, and (d) SON ECMWF reanalysis.

steering flow and, consequently, the number of landfalling systems in North America. Similar findings by Vitart et al. (2001) show that changes in the thermodynamics of the mean tropical background generated by different convection schemes were the main cause for the changes in the tropical storm statistics. Additionally, a test was done on the sensitivity of the value of the tunable diffusion coefficients (temperature, moisture, momentum, and vorticity). The results show that the number of storms in our model was very sensitive to changes in these coefficients. During one experiment, the number of storms increased from 8 to 23 when smaller diffusion coefficients were selected; the observed number of storms was 6. We plan to study these sensitivities further in a future paper.

TABLE 3. Number of storms impacting different sections of the United States from the Zhang and McFarlane (1995) convection scheme (NCAR) and the HURDAT dataset for (June–November) 1986–2005. See Table 2 for a definition of domains and for counting landfalling storms.

Gates	NCAR	HURDAT
TX	21	36
MS/LA	6	11
FL/GA/AL	25	33
Mid-Atlantic	12	11
New England	12	11

6. Summary and conclusions

In this paper, we have examined the use of the FSU–COAPS global model (T126L27) to study the seasonal hindcasting and variability of the western Atlantic hurricane seasons from 1986 to 2005. Weekly observed SSTs were used as lower boundary conditions and time-lagged ECMWF initial conditions were used for the atmosphere. This study used the Vitart et al. (2003) tropical storm detection/tracking algorithm, but it was slightly modified for our higher resolution.

The ensemble members did a remarkable job in reproducing the total number of storms for the 20-yr period: 242, 234, 234, and 249 storms compared to the observed value of 245 storms. The variability in the number of storms was also well captured by the en-

semble mean with a rank correlation of 0.78. The ensemble members also tended to cluster around the ensemble mean during much of the 20 yr. The most notable exception was the El Niño year of 1997 when the ensemble spread was 11 storms; although the ensemble mean was only 2 storms away from the observed. During the cold events of 1998 and 1999, the model overestimated the number of storms with a similar increase in the spread. The model appears sensitive to the ENSO state, although with only 20 yr it is difficult to be quantitatively definite. The model did produce fewer storms during warm events and more storms during cold events, something that is known to occur in the Atlantic. The observed standard deviation during the 20 yr was 5.04, and the ensemble mean was 3.54 with higher standard deviations (greater than 4.0) noted in two of the ensemble members.

The tracks from the ensembles showed that the model tends to move the storms away from the United States too quickly, when observations show that storms come much closer to the eastern seaboard before recurving. These results are an outcome of our atmospheric model's Atlantic large-scale steering flow (approximated by the 500-hPa streamlines). The 500-hPa streamlines show that during the first half of the hurricane season (JJA), the westward flow over the Atlantic tends to turn northeast before it approaches the east coast of the United States because of the break in the high-pressure ridge. The use of a different convection scheme resulted in better landfalling statistics, a result of better large-scale steering flow and the fact that the Zhang and McFarlane (1995) convection scheme generated about 30% more storms than the Hogan and Rosmond (1991) convection scheme. However, the better landfalling statistics did not translate into better interannual storm variability.

As far as intensity, the model was unable to generate storms with surface wind speeds greater than 50 m s^{-1}. Similar findings were noted by Bengtsson et al. (2007a,b) and by Knutson et al. (2007), indicating that it is still difficult even at these high resolutions to produce intense storms. Similarly, this suggests that resolution and perhaps even model physics are still insufficient. Another method of simulating high-horizontal resolution, yet still remaining computationally efficient, is the use of downscaling global model output using regional models (Camargo et al. 2007). These regional models can be downscaled from lower-resolution global models and run for a particular basin of interest.

Based on the limited number of experiments shown here, it remains a question as to whether a different convection scheme could produce more intense storms while still capturing the interannual variability. This study shows that the choice of convection and the choice of the detection criteria are very important in simulating and detecting the interannual variability in the Atlantic. Although not shown here, both convection schemes (Hogan and Rosmond 1991; Zhang and McFarlane 1995) failed to produce high correlations in terms of interannual variability in the western Pacific with correlations on the order of 0.23 for the 20 yr.

One final thought: the results of this paper are encouraging that if given observed weekly updated SSTs, the model can produce the observed interannual variability and total storm numbers with good fidelity. High intensities (defined here as storms greater than 50 m s^{-1}) still remain problematic even for climate models at high horizontal resolutions; hence at this stage, using models at these resolutions (and physics) to study global-warming storm statistics (e.g., changes in intensity) seems premature.

Acknowledgments. We gratefully acknowledge Dr. Frédéric Vitart of ECMWF for providing us with the detection/tracking algorithm. We also wish to thank two anonymous reviewers for their very helpful comments and suggestions on improving the manuscript. We wish to thank Dr. J.J. O'Brien for his continued support. All computations were performed on NCAR's Bluesky supercomputer. COAPS is an NOAA/Applied Research Center funded by the NOAA/Climate Program Office. This research was supported via NOAA Grant NA06OAR4310070.

REFERENCES

Atlas, R., and Coauthors, 2005: Hurricane forecasting with the high-resolution NASA finite volume general circulation model. *Geophys. Res. Lett.,* **32,** L03807, doi:10.1029/2004GL021513.

Bengtsson, L., H. Bottger, and M. Kanamitsu, 1982: Simulation of hurricane-type vortices in a general circulation model. *Tellus,* **34,** 440–457.

——, M. Botzet, and M. Esch, 1995: Hurricane-type vortices in a general circulation model. *Tellus,* **47A,** 175–196.

——, K. I. Hodges, and M. Esch, 2007a: Tropical cyclones in a T159 resolution global climate model: Comparison with observations and re-analyses. *Tellus,* **59A,** 396–416.

——, ——, ——, N. Keenlyside, L. Kornblueh, J.-J. Luo, and T. Yamagata, 2007b: How may tropical cyclones change in a warmer climate? *Tellus,* **59A,** 539–561.

Broccoli, A. J., and S. Manabe, 1990: Can existing climate models be used to study anthropogenic changes in tropical storm climate? *Geophys. Res. Lett.,* **17,** 1917–1920.

Camargo, S. J., and S. Zebiak, 2002: Improving the detection and tracking of tropical storms in atmospheric general circulation models. *Wea. Forecasting,* **17,** 1152–1162.

——, A. Barnston, and S. Zebiak, 2005: A statistical assessment of tropical cyclone activity in atmospheric general circulation models. *Tellus,* **57A,** 589–604.

——, H. Li, and L. Sun, 2007: Feasibility study for downscaling seasonal tropical cyclone activity using the NCEP regional spectral model. *Int. J. Climatol.,* **27,** 311–325.

Chauvin, F., J.-F. Royer, and M. Déqué, 2006: Response of hurricane-type vortices to global warming as simulated by ARPEGE-Climat at high resolution. *Climate Dyn.,* **27,** 377–399.

Cocke, S. D., and T. E. LaRow, 2000: Seasonal predictions using a regional spectral model embedded within a coupled ocean–atmosphere model. *Mon. Wea. Rev.,* **128,** 689–708.

Evans, J. L., 1992: Comment on "Can existing climate models be used to study anthropogenic changes in tropical cyclone climate?" *Geophys. Res. Lett.,* **19,** 1523–1524.

Gray, W. M., 1979: Hurricanes: Their formation, structure, and likely role in the tropical circulation. *Meteorology over the Tropical Oceans,* D. B. Shaw, Ed., Royal Meteor. Soc., 155–218.

——, 1984: Atlantic seasonal hurricane frequency. Part I: El Niño and 30 mb quasi-biennial oscillation influences. *Mon. Wea. Rev.,* **112,** 1649–1668.

——, C. W. Landsea, P. W. Mielke Jr., and K. J. Berry, 1992: Predicting Atlantic seasonal hurricane activity 6–11 months in advance. *Wea. Forecasting,* **7,** 440–455.

——, ——, ——, and ——, 1993: Predicting Atlantic basin seasonal tropical cyclone activity by 1 August. *Wea. Forecasting,* **8,** 73–86.

——, ——, ——, and ——, 1994: Predicting Atlantic basin seasonal tropical cyclone activity by 1 June. *Wea. Forecasting,* **9,** 103–115.

Haarsma, R. J., J. F. B. Mitchell, and C. A. Senior, 1993: Tropical disturbances in a GCM. *Climate Dyn.,* **8,** 247–257.

Hess, J. C., J. B. Elsner, and N. E. LaSeur, 1995: Improving seasonal hurricane predictions for the Atlantic basin. *Wea. Forecasting,* **10,** 425–432.

Hogan, T. F., and T. E. Rosmond, 1991: The description of the Navy Operational Global Atmospheric Prediction System's spectral forecast model. *Mon. Wea. Rev.,* **119,** 1786–1815.

Knutson, T. R., J. Sirutis, S. Garner, I. Held, and R. Tuleya, 2007: Simulation of the recent multidecadal increase of Atlantic hurricane activity using an 18-km-grid regional model. *Bull. Amer. Meteor. Soc.,* **88,** 1549–1565.

LaRow, T. E., and T. N. Krishnamurti, 1998: Initial conditions and ENSO prediction using a coupled ocean–atmosphere model. *Tellus,* **50A,** 76–94.

Lighthill, J., G. Holland, W. Gray, C. Landsea, G. Graig, J. Evans, Y. Kurihara, and C. Guard, 1994: Global climate change and tropical cyclones. *Bull. Amer. Meteor. Soc.,* **75,** 2147–2157.

Manabe, S., J. L. Holloway, and H. M. Stone, 1970: Tropical circulation in a time-integration of a global model of the atmosphere. *J. Atmos. Sci.,* **27,** 580–613.

McDonald, R. E., D. G. Bleaken, D. R. Cresswell, V. D. Pope, and C. A. Senior, 2005: Tropical stroms: Representation and diagnosis in climate models and the impacts of climate change. *Climate Dyn.,* **25,** 19–36.

Oouchi, K., J. Yoshimura, H. Yoshimura, R. Mizuta, S. Kusunoki, and A. Noda, 2006: Tropical cyclone climatology in a global-warming climate as simulated in a 20-km-mesh global atmospheric model: Frequency and wind intensity analyses. *J. Meteor. Soc. Japan,* **84,** 259–276.

Pan, H.-L., and W.-S. Wu, 1994: Implementing a mass-flux convective parameterization package for the NMC Medium-Range Forecast Model. Preprints, *10th Conf. on Numerical Weather Prediction,* Portland, OR, Amer. Meteor. Soc., 96–98.

Reynolds, R. W., N. A. Rayner, T. M. Smith, D. C. Stokes, and W. Wang, 2002: An improved in situ and satellite SST analysis for climate. *J. Climate,* **15,** 1609–1625.

Ryan, B. F., I. G. Watterson, and J. L. Evans, 1992: Tropical cyclone frequencies inferred from Gray's yearly genesis parameter: Validation of GCM tropical climates. *Geophys. Res. Lett.,* **19,** 1831–1834.

Saunders, M. A., and A. R. Harris, 1997: Statistical evidence links exceptional 1995 Atlantic hurricane season to record sea warming. *Geophys. Res. Lett.,* **24,** 1255–1258.

Shapiro, L. J., 1987: Month-to-month variability of the Atlantic tropical circulation and its relationship to tropical storm formation. *Mon. Wea. Rev.,* **115,** 2598–2614.

Thorncroft, C., and I. Pytharoulis, 2001: A dynamical approach to seasonal prediction of Atlantic tropical cyclone activity. *Wea. Forecasting,* **16,** 725–734.

Vitart, F., 2006: Seasonal forecasting of tropical storm frequency using a multi-model ensemble. *Quart. J. Roy. Meteor. Soc.,* **132,** 647–666.

——, and T. Stockdale, 2001: Seasonal forecasting of tropical storms using coupled GCM integrations. *Mon. Wea. Rev.,* **129,** 2521–2537.

——, J. L. Anderson, and W. F. Stern, 1997: Simulation of interannual variability of tropical storm frequency in an ensemble of GCM integrations. *J. Climate,* **10,** 745–760.

——, ——, J. Sirutis, and R. E. Tuleya, 2001: Sensitivity of tropical storms simulated by a general circulation model to changes in cumulus parameterization. *Quart. J. Roy. Meteor. Soc.,* **127,** 25–51.

——, D. Anderson, and T. Stockdale, 2003: Seasonal forecasting of tropical cyclone landfall over Mozambique. *J. Climate,* **16,** 3932–3945.

——, and Coauthors, 2007: Dynamically-based seasonal forecasts of Atlantic tropical storms activity issued in June by EUROSIP. *Geophys. Res. Lett.,* **34,** L16815, doi:10.1029/2007GL030740.

Walsh, K. J. E., M. Fiorino, C. W. Landsea, and K. L. McInnes, 2007: Objectively determined resolution-dependent threshold criteria for the detection of tropical cyclones in climate models and reanalyses. *J. Climate,* **20,** 2307–2314.

Watterson, I. G., J. L. Evans, and B. F. Ryan, 1995: Seasonal and interannual variability of tropical cyclogenesis: Diagnostics from large-scale fields. *J. Climate,* **8,** 3042–3066.

Wu, G., and N.-C. Lau, 1992: A GCM simulation of the relationship between tropical-storm formation and ENSO. *Mon. Wea. Rev.,* **120,** 958–977.

Zhang, G. J., and N. A. McFarlane, 1995: Sensitivity of climate simulations to the parameterization of cumulus convection in the Canadian Climate Centre general circulation model. *Atmos.–Ocean,* **33,** 407–446.